7-2003

Quantitative Air-Coupled Ultrasonic Materials Characterization with Highly Focussed Acoustic Beams

Stephen D. Holland
Iowa State University, sdh4@iastate.edu

Sorin V. Teles
Iowa State University

Dale E. Chimenti
Iowa State University

Quantitative Air-Coupled Ultrasonic Materials Characterization with Highly Focussed Acoustic Beams

Abstract
Plate-wave dispersion spectra have been inferred directly in a single air-coupled coordinate scan using mirror-focussed acoustic beams on both transmitting and receiving transducers. The spectra of the leaky Lamb modes are extracted through a two-dimensional DFT of the measured broadband focused air-coupled signal, as has been demonstrated previously in water. To enhance the typically weak air-coupled signal, a novel signal coding scheme using a random-phase constant-amplitude analog burst 200 μs in length has been employed. Subsequent correlation yields the system impulse response, from which the processed wavenumber-versus-frequency plot is obtained by the two-dimensional DFT. Comparison of measured dispersion spectra with calculated dispersion curves based on nominal stiffness values shows agreement between the measured and calculated data.

Keywords
ultrasonic materials testing, ultrasonic focusing, ultrasonic dispersion, surface acoustic waves, signal processing, ultrasonic transducers, composite materials, aluminium alloys

Disciplines
Aerospace Engineering

This article appeared in *AIP Conference Proceedings*, 700 (2004): 1376–1381 and may be found at http://dx.doi.org/10.1063/1.1711776.

Quantitative AirCoupled Ultrasonic Materials Characterization with Highly Focussed Acoustic Beams

Stephen D. Holland, Sorin V. Teles, and D. E. Chimenti

Citation: AIP Conf. Proc. **700**, 1376 (2004); doi: 10.1063/1.1711776
View online: http://dx.doi.org/10.1063/1.1711776
View Table of Contents: http://proceedings.aip.org/dbt/dbt.jsp?KEY=APCPCS&Volume=700&Issue=1
Published by the American Institute of Physics.

QUANTITATIVE AIR-COUPLED ULTRASONIC MATERIALS CHARACTERIZATION WITH HIGHLY FOCUSSED ACOUSTIC BEAMS

Stephen D. Holland[1], Sorin V. Teles[1], and D. E. Chimenti[2]
[1]Center for NDE, Iowa State Univ, Ames, Iowa 50011
[2]Center for NDE and Aerospace Eng Dept, Iowa State Univ, Ames, Iowa 50011

ABSTRACT. Plate-wave dispersion spectra have been inferred directly in a single air-coupled coordinate scan using mirror-focussed acoustic beams on both transmitting and receiving transducers. The spectra of the leaky Lamb modes are extracted through a two-dimensional DFT of the measured broadband focused air-coupled signal, as has been demonstrated previously in water. To enhance the typically weak air-coupled signal, a novel signal coding scheme using a random-phase constant-amplitude analog burst 200 μs in length has been employed. Subsequent correlation yields the system impulse response, from which the processed wavenumber-versus-frequency plot is obtained by the two-dimensional DFT. Comparison of measured dispersion spectra with calculated dispersion curves based on nominal stiffness values shows agreement between the measured and calculated data.

INTRODUCTION

Ultrasonic testing has long been used for the characterization of mechanical properties of materials. In particular, elastic constants can be calculated directly from measured velocities of ultrasonic waves in a material. Viscoelastic coefficients of the material can be calculated from the measured attenuation in the material. We demonstrate a non-contact method for measuring the dispersion spectrum, and thereby the phase velocities, of Lamb guided modes in plates. The elastic properties of the material can be determined from the dispersion spectra [1]. Our method is based on air-coupled ultrasonic scanning and the synthetic aperture technique of Safaenelli et al. [2].

METHODS

We measure the transmission of a focussed airborne sound beam through a plate as a function of detector position, as shown in Figure 1. The transducer assemblies consist of flat, capacitive air-coupled micromachined transducers [3], attached to custom designed line-focus parabolic mirrors [4], that were constructed directly from CAD drawings using rapid prototyping methods. To measure the Lamb wave dispersion spectrum of the plate, we fix the source transducer assembly and spatially scan the detector transducer assembly in x as we measure the system response to pulse-compressed impulse excitation. This provides a series of time domain waveforms that give voltage as a function of time and space, $V(x,t)$. This series of waveforms contains the entire field of ultrasound transmitted through the plate.

CP700, *Review of Quantitative Nondestructive Evaluation Vol. 23,* ed. by D. O. Thompson and D. E. Chimenti

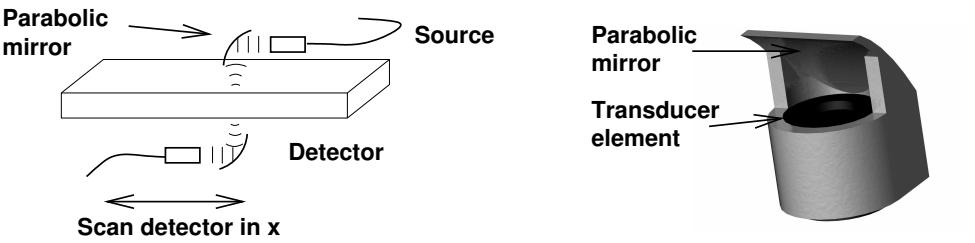

(a) (b)

FIGURE 1. (a) Diagram of measurement apparatus, including transducers, mirrors, and plate. (b) Transducer assembly, including mirror and active element.

Subject to the line-focus assumption, the transmitted field can be analyzed in terms of the transmission coefficient $T(k_x, \omega)$, which is the complex scaling- and phase-factor that represents the effect of the plate on a transmitted airborne plane wave of x wavevector component k_x and angular frequency ω. Because air is such a tenuous coupling medium, its effect upon the Lamb wave structure of the plate is negligible, and therefore the magnitude of the transmission coefficient, $|T(k_x, \omega)|$, can be considered to be a dispersion spectrum. Spatial and temporal Fourier analysis, which we have separately published [5], shows that

$$|V(k_x, \omega)| = \frac{1}{c_a \sqrt{\omega^2/c_a^2 - k_x^2}} |H(k_x, \omega)||T(k_x, \omega)|, \tag{1}$$

where $V(k_x, \omega)$ is the two-dimensional Fourier transform of the measured $V(x, t)$, $H(k_x, \omega)$ is the combined effect including shape, spectrum, and focussing of the transducers, and $T(k_x, \omega)$ is the transmission coefficient. The magnitude of the two-dimensional Fourier transform of the measured waveforms is equal to the transmission coefficient and hence the dispersion spectrum, subject to a scaling factor and the multiplicative spectral sensitivity window of the transducers. On this basis, by computing the discrete two-dimensional Fourier transform of the measured $V(x, t)$ impulse-response data, we can determine the dispersion spectrum of the plate.

The effect of the transducers, $H(k_x, \omega)$ can be determined by performing a scan and transform with the plate removed. In this case, $T(k_x, \omega) = 1$, so

$$|V(k_x, \omega)| = \frac{1}{c_a \sqrt{\omega^2/c_a^2 - k_x^2}} |H(k_x, \omega)|.$$

A spatial scan of the impulse response $V(x, t)$ with the plate removed, Fourier transformed to $V(k_x, \omega)$, yields the transducer behavior $H(k_x, \omega)$, scaled by $1/c_a \sqrt{\omega^2/c_a^2 - k_x^2}$. Figure 2a shows the measured spectral transducer response. It reveals sensitivity between 50 and 450 kHz over an angular range of 14.4°. The sensitivity range of the transducer limits the region in (k_x, ω) which can be measured. Fig. 2b illustrates the effect of the sensitivity region with a scan of 5.46-mm Lucite. The dispersion spectrum is only measured between the two straight white lines, which correspond to the sensitivity boundaries of the focussed transducers. For most measurements, we will rotate the transducers so as to increase the portion of the right-half plane within the sensitivity window.

We use pulse compression [6] to measure the impulse response at each detector position x. Instead of using an actual impulse source, our source is a 190 μs long waveform that

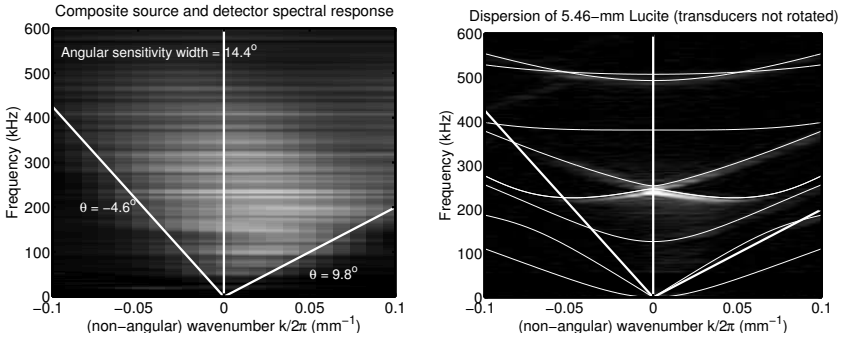

FIGURE 2. (a) Spectral sensitivity window of the combined source and detector transducers. White lines represent the $k = 0$ axis and the bounds of the sensitivity region. (b) Effect of sensitivity window on a dispersion spectrum. Calculated dispersion curves are superimposed.

has uniform spectral amplitude over our desired range but random phase. The waveform is generated by an iterative algorithm that repeatedly alternately applies inherently inconsistent time- and frequency-window criteria to randomly generated phase noise, until both the time and frequency criteria are nearly satisfied. The measured response waveforms to this excitation are cross-correlated with the excitation waveform to yield the pulse-compressed impulse response. With pulse compression, much more incident energy can be used to probe the sample than with impulse excitation, because that energy can be spread out over a much longer time without sacrificing either bandwidth or time resolution. The random phase excitation provides a broadband spectrum for the pulse compression algorithm, while eliminating time-domain nonlinearity artifacts.

RESULTS

We have performed a series of dispersion measurements on different samples, and find almost perfect matches between measured dispersion spectra and the dispersion relations calculated from nominal elastic constants and Lamb wave theory. Figure 3 shows a 100 kHz - 800 kHz measured dispersion spectrum for 6.68-mm Aluminum. The transducers were rotated to 2° to allow measurement of a wider range of modes. Pulse-compressed impulse-response measurements were performed over a distance of 300 mm in 2-mm steps. These time-domain signals were windowed to eliminate multiple echos and 2D discrete Fourier transformed to yield the dispersion spectrum in Fig. 3. Dispersion curves calculated from Lamb wave theory are superimposed over the dispersion spectrum as dashed lines. We observe an almost perfect match between the calculated curves and measure spectrum. Some modes appear brighter than others on the dispersion spectrum. This is in part because of the limited spectral and angular sensitivity window of the transducer system (Fig. 2), but also because of the difference in coupling between modes. For example, the lower section of the lowest order symmetric mode (second from the bottom on Fig. 3) at frequencies below 0.3 MHz shows much less coupling than the segment beyond 0.3 MHz. This is because the vertical displacements of that mode are much smaller in the lower frequency segment than in the higher frequency segment, and hence air-coupling is more efficient in the higher frequency segment.

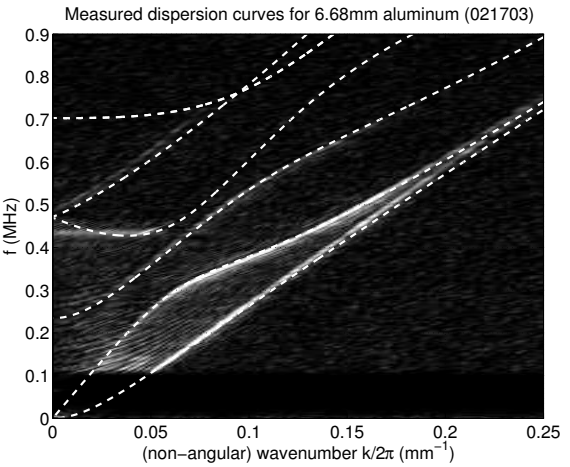

FIGURE 3. Measured dispersion spectrum of 6.68-mm Aluminum, with calculated dispersion relation superimposed as dashed lines.

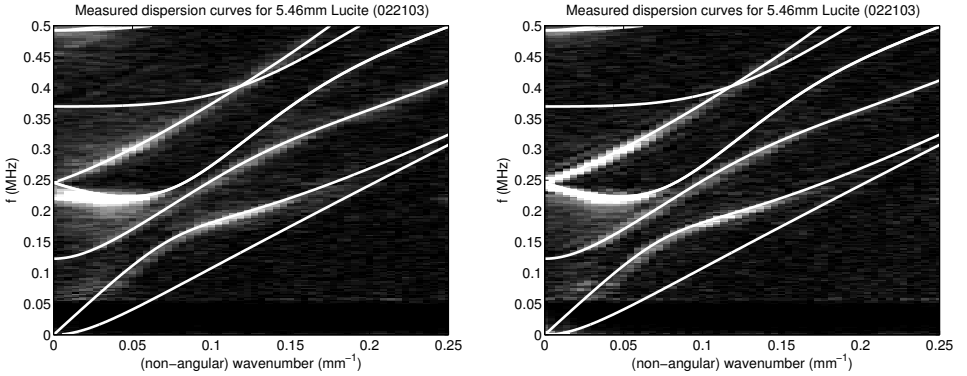

FIGURE 4. (a) Dispersion scan of 5.46-mm Lucite, 2D analysis, with superimposed calculated curves. (b) 3D analysis.

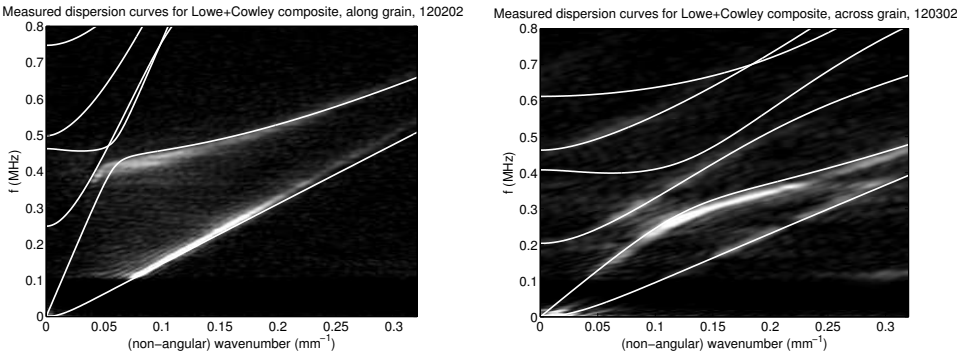

FIGURE 5. (a) Measured dispersion spectrum for 3.3-mm uniaxial composite, measured parallel to fibers. Calculated dispersion curves are superimposed. (b) Measured across fibers.

Figure 4a shows the results of a dispersion scan of a 5.46-mm Lucite plate, with calculated curves superimposed. Once again, the measured dispersion spectrum and calculated dispersion curves agree almost perfectly. However, at the bright spot at 220 kHz the agreement is not so good. An imperfect match is also visible at the corresponding location on Fig. 3. This is near the zero-group-velocity point, which appears as a relative minimum in the dispersion relation, of the first order symmetric (S_1) mode. We have discovered, and discuss elsewhere in these proceedings [7], a phenomenon of strong transmission at the zero-group-velocity point. In this region, near the $k_x = 0$ axis, our line-focus transducers are too narrow to behave purely as line-focus. The bright spot in Fig. 4a appears in the wrong place because of wave propagation out of the measurement plane, and this is exacerbated by the relatively efficient coupling of the S_1 mode at this point. If we extend our analysis to three dimensions, by performing a 2D $V(x, y, t)$ spatial scan and three dimensional Fourier transform to $V(k_x, k_y, \omega)$, then we obtain (at $k_y = 0$) the spectrum in Fig. 4b. This is identical to Fig. 4a, except that the bright spot at 220 kHz now appears along the dispersion curve, where it would be expected.

Our method is not limited to measuring the dispersion spectra of isotropic samples. Figure 5 shows dispersion scans of a 3.3-mm thick uniaxial carbon fiber epoxy laminate. Figure 5a shows a scan of propagation parallel to the fiber direction, while Fig. 5b shows a scan of propagation across the fiber direction. The superimposed dispersion curves were calculated based on independently measured elastic constants. For parallel propagation, we can clearly see the lowest order antisymmetric and symmetric modes. For propagation across the fiber direction, we see the lowest order symmetric and antisymmetric modes, but we also see the first order antisymmetric and the second order symmetric modes. The across-fiber curves look quite similar to those for isotropic samples because they correspond to propagation in the plane of isotropy of a transversely isotropic sample.

CONCLUSIONS

We have discussed and demonstrated a non-contact air-coupled method for the measurement of Lamb wave dispersion spectra in isotropic and anisotropic plates. This method simultaneously measures over a wide range of angles and frequencies by probing with a fo-

cussed, broadband impulse. The measured dispersion spectra consolidate information about the material parameters along the axis of measurement into a single image, and allow direct comparison of measured dispersion with calculated curves. The high sensitivity of specific dispersion curve segments to particular elastic constants is well established [1, 8], and therefore these dispersion spectra provide quantitative information about the elastic constants. We have measured a variety of samples and shown agreement between measured dispersion spectra and dispersion curves calculated from independently measured elastic parameters.

ACKNOWLEDGMENTS

This material is based on work supported by NASA under award NAG-1-029098.

REFERENCES

1. D. Fei and D. E. Chimenti, "Single-scan elastic property estimation in plates," Acoustics Res. Lett. Online **2**, 49-54 (2001)

2. A. Safaeinili, O. I. Lobkis, D. E. Chimenti, "Air-coupled ultrasonic estimation of viscoelastic stiffness in plates," IEEE Trans. Ultrason. Ferro. Freq. Control **43**, 1171-1180 (1996)

3. D. W. Schindel, D. A. Hutchins, L. Zou, and M. Sayer, "The design and characterization of micromachined air-coupled capacitance transducers," IEEE Trans. Ultrason. Ferroelec. Freq. Control, **42**, 42-50 (1995)

4. B. Hosten and M. Castaings, "Parabolic mirror and air-coupled transducer for multimodal plate wave detection," in *Review of Progress in Quantitative Nondestructive Evaluation*, vol. 22, eds. D. O. Thompson and D. E. Chimenti (AIP Press, New York, 2002), pp 1243-1250.

5. S. D. Holland, S. V. Teles, and D. E. Chimenti, "Air-coupled, focussed ultrasonic dispersion spectrum reconstruction in plates," Submitted for publication, J. of the Acoust. Soc. of Amer. (2003)

6. T. H. Gan, D. A. Hutchins, D. R. Billson, D. W. Schindel, "The use of broadband acoustic transducers and pulse-compression techniques for air-coupled ultrasonic imaging," Ultrasonics **39** 181-194 (2001).

7. Stephen D. Holland, and D. E. Chimenti, "High-sensitivity air-coupled ultrasonic imaging with the first-order symmetric Lamb mode at zero group velocity," presented at *QNDE 2003*, July 27-August 1, 2003, Green Bay, Wisconsin.

8. D. E. Chimenti and D. Fei, "Scattering coefficient reconstruction in plates using focussed acoustic beams," International Journal of Solids and Structures **39**, 5495 (2002).